NASA TECHNICAL MEMORANDUM

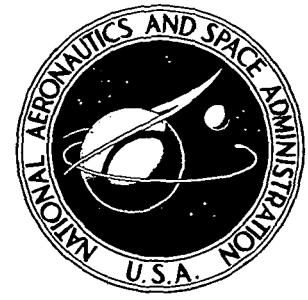

NASA TM X-3271 C.1

NASA TM X-3271

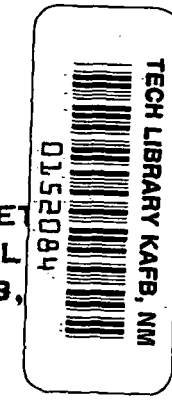

EFFECT OF THERMAL CYCLING IN A MACH 0.3 BURNER RIG ON PROPERTIES AND STRUCTURE OF DIRECTIONALLY SOLIDIFIED γ/γ'-δ EUTECTIC

Hugh R. Gray and William A. Sanders

Lewis Research Center

Cleveland, Ohio 44135

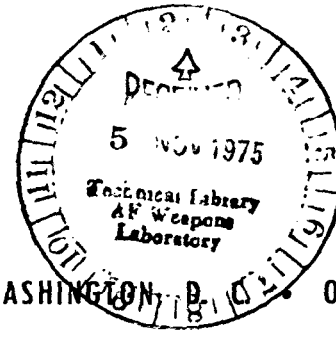

NATIONAL AERONAUTICS AND SPACE ADMINISTRATION • WASHINGTON, D. C. • OCTOBER 1975

1. Report No.	2. Government Accession No.	3. Recipient's Catalog No.
NASA TM X-3271		

4. Title and Subtitle	5. Report Date
EFFECT OF THERMAL CYCLING IN A MACH 0.3 BURNER RIG ON PROPERTIES AND STRUCTURE OF DIRECTIONALLY SOLIDIFIED γ/γ' - δ EUTECTIC	October 1975
	6. Performing Organization Code
7. Author(s)	8. Performing Organization Report No.
Hugh R. Gray and William A. Sanders	E-8272
	10. Work Unit No.
9. Performing Organization Name and Address	505-01
Lewis Research Center National Aeronautics and Space Administration Cleveland, Ohio 44135	11. Contract or Grant No.
	13. Type of Report and Period Covered
12. Sponsoring Agency Name and Address	Technical Memorandum
National Aeronautics and Space Administration Washington, D.C. 20546	14. Sponsoring Agency Code

15. Supplementary Notes

16. Abstract

Tensile and stress rupture properties at 1040° C of a thermally cycled γ/γ' - δ eutectic were essentially equivalent to the as-grown properties. Tensile strength and rupture life at 760° C appeared to have been decreased slightly by thermal cycling. Thermal cycling resulted in gamma prime coarsening and Widmanstätten delta precipitation in the gamma phase. An unidentified precipitate, presumably gamma prime, was observed within the delta phase. The eutectic alloy exhibited a high rate of oxidation-erosion weight loss during thermal cycling in the Mach 0.3 burner rig.

17. Key Words (Suggested by Author(s))	18. Distribution Statement
Eutectic alloys; Directionally solidified eutectics; High-temperature turbine alloys; Gamma/gamma prime - delta eutectic; Thermal cycling stability; Oxidation	Unclassified - unlimited STAR Category 26 (rev.)

19. Security Classif. (of this report)	20. Security Classif. (of this page)	21. No. of Pages	22. Price*
Unclassified	Unclassified	31	$3.75

* For sale by the National Technical Information Service, Springfield, Virginia 22161

Page Intentionally Left Blank

EFFECT OF THERMAL CYCLING IN A MACH 0.3 BURNER RIG ON PROPERTIES AND STRUCTURE OF DIRECTIONALLY SOLIDIFIED $\gamma/\gamma' - \delta$ EUTECTIC*

by Hugh R. Gray and William A. Sanders

Lewis Research Center

SUMMARY

This investigation was conducted to determine the effect of thermal cycling on the mechanical properties parallel to the growth direction and on the microstructure of a directionally solidified gamma/gamma prime - delta ($\gamma/\gamma' - \delta$) eutectic alloy. The alloy had a composition of Ni-20Cb-6Cr-2.5Al and had been directionally solidified at a rate of 3 centimeters per hour. Test bars were exposed in an oxidation-erosion burner rig at a gas velocity of Mach 0.3. Bars were heated to 1100° C, held at that temperature for 1 minute, and then cooled to 425° C. The elapsed time of each cycle was 2.5 minutes and a total of 3000 cycles were applied to the bars.

Thermal cycling of $\gamma/\gamma' - \delta$ resulted in gamma prime coarsening and Widmanstätten delta precipitation in the gamma phase. An unidentified precipitate, presumably gamma prime, was observed within the delta phase. However, these microstructural changes did not result in any substantial changes in the mechanical properties of the alloy. Tensile and stress rupture properties at 1040° C of thermally cycled material were essentially equivalent to the as-grown properties. The tensile ductility and rupture ductility at 760° C of thermally cycled $\gamma/\gamma' - \delta$ were also essentially equivalent to the as-grown ductilities. The tensile strength at 760° C was about 8 percent lower than that determined for as-grown $\gamma/\gamma' - \delta$. The rupture life at 760° C appeared to have been slightly decreased by thermal cycling, although the scatter for as-grown specimens prevented a firm conclusion that thermal cycling is detrimental.

The $\gamma/\gamma' - \delta$ alloy exhibited a high rate of oxidation-erosion weight loss during thermal cycling in the Mach 0.3 burner rig, thus confirming the previously recognized requirement for protective coatings.

This investigation has demonstrated that tensile and stress rupture properties of the directionally solidified $\gamma/\gamma' - \delta$ eutectic were relatively unaffected by the microstructural changes that occurred during cyclic thermal exposure. These results offer additional confirmation of the potential of $\gamma/\gamma' - \delta$ eutectic alloy for advanced turbine components.

---

*A condensed version of this material was presented at the Conference on In Situ Composites-II, Bolton Landing, New York, September 2-5, 1975.

INTRODUCTION

A directionally solidified gamma/gamma prime - delta ($\gamma/\gamma' - \delta$) eutectic alloy (Ni-20Cb-6Cr-2.5Al) has been shown to have considerable potential as a turbine blade and vane material in advanced aircraft gas turbine engines. The $\gamma/\gamma' - \delta$ alloy offers an increase of about 50° C in use temperature and a 50 percent increase in strength at current airfoil operating temperatures compared with current alloys (ref. 1). The higher use-temperature capability would permit an increase in turbine inlet gas temperature over current levels without compromising engine performance with additional cooling air. The higher strength of the alloy at existing blade metal temperatures would permit an increase in rotor speed, which would also contribute to increased engine performance.

In addition to these properties, turbine blade alloys must have other characteristics, such as cyclic oxidation resistance, thermal fatigue resistance, and thermal stability. A previous investigation (ref. 2) has shown that the $\gamma/\gamma' - \delta$ alloy has only marginal oxidation resistance in static air under isothermal and cyclic conditions. However, protective coatings are being developed to satisfactorily protect the alloy (ref. 3). The thermal fatigue characteristics of the $\gamma/\gamma' - \delta$ alloy are currently under investigation (ref. 4). Limited data at elevated temperatures have indicated that the alloy has excellent thermal stability in static air under isothermal and cyclic (self-resistively heated) conditions (refs. 5 to 7).

The purpose of this investigation was to examine in more detail the effect of cyclic thermal exposures on the mechanical properties of $\gamma/\gamma' - \delta$ parallel to the growth direction. Bars of the alloy were exposed in a Mach 0.3 burner rig and cycled 3000 times between 1100° and 425° C. Oxidation-erosion characteristics of the alloy were determined by weight loss measurements at 300-cycle intervals. After cyclic exposure, stress rupture and tensile tests were conducted at both 760° and 1040° C. Microstructural changes resulting from this cyclic exposure were also determined.

MATERIAL, SPECIMENS, AND PROCEDURE

Material

The gamma/gamma prime - delta ($\gamma/\gamma' - \delta$) eutectic alloy used throughout this investigation was produced by United Technologies Research Center (UTRC). The alloy had a nominal composition by weight of Ni-20Cb-6Cr-2.5Al. It was directionally solidified at a rate of 3 centimeters per hour in a modified Bridgeman furnace having a thermal gradient of at least 200° C per centimeter (ref. 2). Each heat resulted in a

casting approximately 20 centimeters in length and 1.2 centimeters in diameter. The casting was then cut into two bars each approximately 7.5 centimeters long.

The tensile and stress rupture data determined both before and after burner rig exposure are given in tables I to III. Specimens are identified by heat number (A73-xxx and A74-xxx) and bar location. The bottom bar from each casting is identified as "01" and the top bar from each casting is identified as "02."

Metallographic screening of a transverse section of all bars by UTRC assured a minimum of 75-volume-percent alined lamellar structure. Starting with heat number A74-234, a longitudinal flat on each bar was macroetched by UTRC to assure alined structures. All bars were inspected at NASA by both dye penetrant and X-ray techniques to ensure soundness.

Specimens

NASA taper-headed specimens (ref. 8) were used for both tensile and stress rupture testing (fig. 1). All specimens were oriented parallel to the growth direction of the directionally solidified bars. Machined specimens were also inspected by both dye penetrant and X-ray techniques to ensure soundness. Initial mechanical tests were conducted with short and medium-length specimens to conserve material. However, occasional partial shearing of specimen heads demonstrated the need for heavier heads. Thus, a 7.1-centimeter-long specimen was used for the bulk of the mechanical testing. With the exception of one specimen in which the head sheared off completely, the partially sheared specimens failed in the gage section and the tests were considered valid.

Test Procedure

Burner rig exposure. - The 7.5-centimeter-long, 1.2-centimeter-diameter cylindrical test bars were exposed to thermal cycling in a Mach 0.3 gas velocity burner rig. Batches of eight bars were heated in the combustion gases resulting from the burning of a mixture of Jet A grade fuel and air. While being exposed the bars were rotated in a sample holder at 450 rpm to ensure uniform temperatures. Bars were heated to 1100° C, held at that temperature for 1 minute, and then cooled to 425° C with a Mach 0.7 blast of room-temperature air. The elapsed time for each cycle was 2.5 minutes. All bars were cycled a total of 3000 times. The equipment was shut down after every 300 cycles, and the test bars were weighed to permit determination of the cyclic oxidation-erosion rate. The bars were exposed for 3000 cycles in three separate batches, as identified in table III. Specimens were then machined from the exposed bars.

Tensile testing. - Tensile tests were conducted on as-grown specimens over the temperature range 23° to 1040° C to determine baseline properties. Tensile tests of thermally cycled specimens were conducted at 760° and 1040° C. Tests were done in air at a crosshead speed of 0.05 centimeter per minute. All tensile test results are listed in tables I and III.

Stress rupture testing. - Rupture properties of as-grown specimens were determined over the temperature range 675° to 1040° C at stresses of 895 to 140 MN/m^2 (130 to 20 ksi). Most tests were performed in air, but a few tests were conducted in helium. The effect of thermal cycling was determined by rupture testing at 760° and 1040° C at stresses of 760 and 150 MN/m^2 (110 and 22 ksi), respectively. Results of the stress rupture tests are listed in tables II and III. All tensile and rupture elongation data were determined by first measuring the total length of the fractured specimen. Then elongation was calculated by assuming that deformation occurred only over the gage length.

RESULTS AND DISCUSSION

Effect of Cyclic Exposure on Properties

Tensile properties. - The tensile strength and elongation of $\gamma/\gamma' - \delta$ bars after 3000 cycles in the burner rig are shown in figure 2. Baseline properties of as-grown (as directionally solidified) $\gamma/\gamma' - \delta$ are also shown for comparative purposes. It appears that the tensile strength at 760° C has been decreased slightly - from about 1050 MN/m^2 (152 ksi) for as-grown material to about 965 MN/m^2 (140 ksi) for thermally cycled material. Elongations at 760° C for thermally cycled and as-grown material were essentially equivalent. Likewise, both tensile strength and elongation at 1040° C for thermally cycled and as-grown material were essentially equivalent.

Stress rupture properties. - The effect of thermal cycling on the stress rupture properties of $\gamma/\gamma' - \delta$ was determined by testing thermally cycled specimens at 760° and 1040° C at stresses of 760 and 150 MN/m^2 (110 and 22 ksi), respectively. The results are shown in figure 3(a) for rupture life and in figure 3(b) for rupture elongation, together with comparative data for as-grown $\gamma/\gamma' - \delta$. Neither rupture life nor rupture elongation at 1040° C was significantly affected by thermal cycling. Rupture elongation at 760° C of thermally cycled material was also approximately the same as that of as-grown $\gamma/\gamma' - \delta$.

As shown in figure 3(a), there appeared to be a slight decrease in rupture life at 760° C for thermally cycled material as compared with as-grown material. However, since a significant degree of scatter occurred for the rupture lives of as-grown mate-

rial (table II), it cannot be stated with certainty that thermal cycling has a detrimental effect on rupture life. The cause of scatter in rupture lives near 760° C is being investigated.

A few rupture tests on as-grown material were conducted at 760° and 1040° C in helium and are noted in table II. At 760° C, no difference in rupture life was observed for tests run in air and tests run in helium. At 1040° C the rupture lives of specimens run in helium were slightly longer (approximately 10 percent) than those run in air.

Although a large number of rupture specimens failed near the end of the gage length (table II), such failure was not consistently associated with short or long rupture life. For example, several specimens with extremely long lives failed near the end of the gage length (specimen shown in fig. 4 and other specimens listed in table II). Likewise, several specimens with extremely short lives failed near midgage (specimen shown in fig. 5 and other specimens in table II).

Metallographic evaluation. - Metallographic examinations of as-grown specimens (figs. 4 and 5) and thermally exposed specimens (figs. 6 to 11) after rupture or tensile testing revealed the following. The top (02) specimens (figs. 5, 7, 9, and 11) had larger amounts of primary delta phase than did the bottom (01) specimens (figs. 4, 6, 8, and 10). However, the occurrence of primary delta had no consistent effect on mechanical properties. For example, top specimens had shorter rupture lives at 760° C (compare fig. 5 with fig. 4) and poorer tensile strength at 760° C (compare fig. 11 with fig. 10) than did bottom specimens. In another case a top specimen had a longer rupture life at 760° C than did the corresponding bottom specimen (compare fig. 7 with fig. 6). In still another case a bottom specimen with a well-alined, delta-free microstructure (fig. 8) had a rupture life at 1040° C equivalent to that of the corresponding top specimen with a highly cellular, delta-containing microstructure (fig. 9).

Effect of Cyclic Exposure on Microstructure

Since the exhaust gases of the Mach 0.3 burner rig impinge on only the upper portion of the test bars, a temperature gradient obviously exists along the length of the bars. Such a temperature gradient might be expected to result in a gradient in microstructural features along the length of the bars. It was also considered possible that certain microstructural changes could result in changes in mechanical properties of the $\gamma/\gamma' - \delta$ alloy. The next sections of this report consider these aspects of cyclic exposures.

Tensile and rupture failure locations. - The approximate temperature gradient existing along the length of a test bar exposed in the burner rig (ref. 8) is shown in figure 12. The upper half of the bar is at or close to the nominal test temperature of

1100° C. However, a very steep temperature gradient occurs in the lower portion of the bar. Since a portion of the gage section of the machined test specimen corresponds with the location of the temperature gradient, failure locations of all exposed specimens are noted (table III and fig. 12).

It is evident that the fracture locations along the specimen gage length for both tensile and rupture specimens tested at both 760° and 1040° C follow no consistent pattern which might be related to the formation of a detrimental phase in a specific temperature range.

Metallographic evaluations. - In addition to the metallography performed on fractured specimens (figs. 6 to 11), one test bar that had been exposed in the burner rig was examined at eight transverse locations along its length (fig. 12). These transverse photomicrographs and selected longitudinal photomicrographs are presented in figure 13. The approximate temperature that occurred during cyclic exposure is also indicated for each of the locations.

Maximum gamma prime coarsening was observed at locations 2 and 3 (approximately 1100° C), as shown in figures 13(b) to (d). Slightly less gamma prime coarsening was observed at locations 1, 4, and 5 (approximately 1070° to 1100° C), as shown in figure 13(a) and (e) to (h). Widmanstätten delta precipitation was observed in the gamma phase at locations 1 to 7 (900° to 1100° C), primarily in cellular regions (fig. 13(f)) but also in interlamellar regions. An unidentified precipitate, presumably gamma prime, was observed at locations 1 to 6 (1000° to 1100° C) within the delta phase (figs. 13(a) to (i)).

Because precise temperatures along the length of a bar could not be reliably controlled in the burner rig, a detailed investigation of microstructural changes and corresponding exposure temperatures was not attempted in this investigation. However, such a study has been performed in a parallel investigation (unpublished work by S. N. Tewari, R. L. Dreshfield, and C. W. Andrews of Lewis).

Cyclic Oxidation-Erosion Behavior

Weight loss determinations. - The results of weight loss measurements made at 300-cycle increments are shown in figure 14 for uncoated $\gamma/\gamma' - \delta$. The alloy exhibited an average rate of oxidation-erosion weight loss of approximately 0.08 mg/(cm^2) (cycle). The weight losses for individual bars fell within the scatter bands shown in figure 14. Good reproducibility was noted for two different test runs (compare batch 1 with batch 2).

For comparative purposes, data for uncoated B-1900 determined under a similar

but slightly more severe thermal cycle (unpublished work by C. A. Barrett, J. R. Johnston, and W. A. Sanders of Lewis) are also shown in figure 14. It is immediately evident that the oxidation-erosion resistance of $\gamma/\gamma' - \delta$ is substantially poorer than that of B-1900. This poor oxidation-erosion resistance of $\gamma/\gamma' - \delta$ was not unexpected and, indeed, previous test results conducted in static air indicated that protective coatings will be required for reliable service of $\gamma/\gamma' - \delta$ (ref. 2).

Metallographic evaluation. - The appearance of the test bars after 1500 and 3000 cycles is shown in figure 15. It is evident that severe oxide spallation has occurred in a fairly uniform manner on the top half of each bar. A diametral change of 0.62 millimeter was measured in the middle of the hot zone for one of the bars after 3000 cycles. A decrease in diameter is evident in figure 15 and is also indicated in figure 16. A transverse metallographic section through the middle of the hot zone (fig. 16) indicates an oxide thickness of about 50 micrometers, considerable cracking in the oxide surface layer, and an alloy depletion zone 10 to 20 micrometers thick. Measured metal loss is in good agreement with that previously reported for cyclic oxidation in static air (ref. 2).

X-ray diffraction evaluation. - Surface X-ray diffraction analysis in the middle of the hot zone of a bar exposed for 3000 cycles revealed very strong patterns for NiO and $CrCbO_4$ and a medium-strength pattern for $NiCb_2O_6$. Results of a previous study (ref. 2) in static air indicated the presence of NiO, $CrCbO_4$, and also Cr_2O_3 and α-Al_2O_3.

The absence of Cr_2O_3 and Al_2O_3 in this study is probably due to the more severe dynamic oxidation environment characteristic of the Mach 0.3 burner rig. The rapid heating and cooling rates and the erosive effect of the high-velocity gas stream would augment spalling and thus result in the loss of Cr_2O_3 and Al_2O_3. In addition, loss of Cr_2O_3 from vaporization would be expected to be more pronounced in the high-velocity gas stream (ref. 9).

SUMMARY OF RESULTS

The purpose of this investigation was to determine the effect of thermal cycling on the mechanical properties parallel to the growth direction and on the microstructure of a gamma/gamma prime - delta ($\gamma/\gamma' - \delta$) directionally solidified eutectic alloy. This alloy had a composition of Ni-20Cb-6Cr-2.5Al and had been solidified at a rate of 3 centimeters per hour. Bars of the alloy were exposed in an oxidation-erosion burner rig at a gas velocity of Mach 0.3. Bars were heated to 1100° C, held at that temperature for 1 minute, and then cooled to 425° C. Elapsed time of each cycle was 2.5 minutes and a total of 3000 cycles were applied to the bars. Cyclic oxidation-erosion weight losses were measured. Tensile and stress rupture properties of the thermally

cycled alloy were determined at both 760° and 1040° C and compared with baseline properties of the as-grown (as directionally solidified) alloy. Microstructural changes due to thermal cycling were also determined. The following results were obtained:

1. Thermal cycling of $\gamma/\gamma' - \delta$ resulted in gamma prime coarsening and Widmanstätten delta precipitation in the gamma phase. An unidentified precipitate, presumably gamma prime, was observed within the delta phase. However, these microstructural changes did not have any substantial effects on the mechanical properties of $\gamma/\gamma' - \delta$.

2. Both the tensile and stress rupture properties at 1040° C of thermally cycled $\gamma/\gamma' - \delta$ were essentially equivalent to the properties of the as-grown material.

3. The tensile ductility and rupture ductility at 760° C of thermally cycled $\gamma/\gamma' - \delta$ were also approximately equal to those of as-grown $\gamma/\gamma' - \delta$. The tensile strength at 760° C was approximately 8 percent lower for thermally exposed material. The rupture life at 760° C appeared to have been decreased by thermal cycling, although the large amount of scatter in as-grown data prevents a firm conclusion regarding the detrimental effect of thermal cycling.

4. The $\gamma/\gamma' - \delta$ alloy exhibited a high rate of oxidation-erosion weight loss during thermal cycling in the Mach 0.3 burner rig, thus confirming the need for protective coatings to ensure reliable service as turbine blades.

Lewis Research Center,
National Aeronautics and Space Administration,
Cleveland, Ohio, July 1, 1975,
505-01.

REFERENCES

1. Gell, M.; and Donachie, M. J.: Directionally Solidified Eutectics for Use in Advanced Gas Turbine Engines. Materials on the Move; Proc. Sixth Nat. Tech. Conf., Soc. for Advancement of Mat. and Process Eng., 1974, pp. 188-195.

2. Lemkey, F. D.: Eutectic Superalloys Strengthened by δ, Ni_3Cb Lamellae and γ', Ni_3Al Precipitates. NASA CR-2278, 1973.

3. Felten, E. J.; Strangman, T. E.; and Ulion, N. E.: Coatings for Directional Eutectics. (PWA-5091, Pratt & Whitney Aircraft; NAS3-16792), NASA CR-134735, 1974.

4. Sheffler, K. D.; and Barkalow, R. H.: Alloy and Structural Optimization of a Directionally Solidified Lamellar Eutectic Alloy. Pratt & Whitney Aircraft (NAS3-17811), 1975.

5. Breinan, E. M.; Thompson, E. R.; and Lemkey, F. D.: The Effect of Thermal Cycling on High Temperature Eutectic Composites. Proc. Conf. on In Situ Composites, vol. 2, Natl. Res. Council, 1972, pp. 201-213.

6. Gell, M.: Thermal Stability of Directionally Solidified Composites. Specialists Meeting on Directionally Solidified In-Situ Composites, E. R. Thompson and P. R. Sahm, eds., AGARD-CP-156, 1974, pp. 117-124.

7. Lemkey, F. D.; and McCarthy, G.: Quaternary and Quinary Modifications of Eutectic Superalloys Strengthened by δ, Ni_3Cb Lamellae and γ', Ni_3Al Precipitates. (R911698-13, United Aircraft Corp.; NAS3-17785), NASA CR-134678, 1975.

8. Dunlevey, F. M.; and Wallace, J. F.: The Effect of Thermal Cycling on the Structure and Properties of a Co, Cr, Ni-TaC Directionally Solidified Eutectic Composite. (Case Western Reserve Univ.; NGR-36-027-035), NASA CR-121249, 1973.

9. Wasielewski, Gerald E.; and Rapp, Robert A.: High Temperature Oxidation. Ch. 10 of The Superalloys - Vital High Temperature Gas Turbine Materials for Aerospace and Industrial Power, Chester T. Sims and William C. Hagel, eds., John Wiley & Sons, 1972, pp. 287-316.

TABLE I. - TENSILE TEST DATA OF AS-GROWN $\gamma/\gamma' - \delta$

Specimen	Temperature, °C	Ultimate tensile strength		Reduction of area, percent	Elongation, percent
		MN/m^2	ksi		
A74-003-01	23	1225	178	5	5
003-02	23	1220	177	5	5
A73-891-01	650	1160	168	10	8
891-02	650	1150	167	9	8
811-01	760	1040	151	22	9
811-02	↓	1050	152	10	7
A74-612-01		1055	153	22	13
[a]024-02		1025	149	11	8
A73-817-01	870	910	132	15	6
817-02	870	895	130	16	6
A74-154-02	925	805	117	4	[d]2
225-01	925	840	122	6	3
292-01	980	765	111	9	6
300-01	980	760	110	8	7
[b]A73-638-02	1040	---	---	--	--
[c]643-02	↓	635	92	19	16
A74-018-01		650	94	24	12
018-02		660	96	9	6

[a]Tensile crosshead speed, 0.005 cm/min; all others 0.05 cm/min.

[b]Short specimen - total head shear.

[c]Medium-length specimen - partial head shear.

[d]Failed near end of gage section.

TABLE II. - STRESS RUPTURE DATA OF AS-GROWN $\gamma/\gamma' - \delta$

Specimen	Temperature, °C	Stress		Rupture life, hr	Reduction of area, percent	Elongation, percent
		MN/m^2	ksi			
A74-024-01	675	895	130	243	4	3
111-01	↓	↓	↓	301	4	[i]1
527-01	↓	↓	↓	423	4	2
527-02	↓	↓	↓	898	2	2
425-01	760	795	115	116	2	[i]2
498-01	↓	795	115	53	2	[i]1
498-02	↓	795	115	123	1	[i]2
[a, b, c]A73-638-01	↓	760	110	31	5	[i]1
[c, d]643-01	↓	↓	↓	264	2	[i]2
[d]755-01	↓	↓	↓	235	3	[i]2
755-02	↓	↓	↓	441	1	[i]3
[c]782-01	↓	↓	↓	140	3	[i]2
[c, e]782-02	↓	↓	↓	---	5	4
890-01	↓	↓	↓	438	2	[i]2
890-02	↓	↓	↓	7	12	9
[c]897-01	↓	↓	↓	129	2	[i]4
[c]897-02	↓	↓	↓	197	2	[i]3
A74-623-01	↓	↓	↓	89	2	[i]1
453-02	↓	690	100	2012	3	[i]5
462-01	↓	↓	↓	126	1	[i]2
546-01	↓	↓	↓	14	12	8
546-02	↓	↓	↓	150	1	[i]1
462-02	800	↓	↓	426	5	[i]6
467-02	800	↓	↓	284	4	[i]5
467-01	800	635	92	77	2	1
[f]206-01	870	565	82	1	31	15
206-02	↓	↓	↓	79	8	[i]5
509-01	↓	↓	↓	76	21	10
509-02	↓	↓	↓	11	1	[i]2

Specimen	Temperature, °C	Stress		Rupture life, hr	Reduction of area, percent	Elongation, percent
		MN/m^2	ksi			
A74-518-01	870	565	82	75	23	11
518-02	↓	565	82	78	17	11
A73-827-01	↓	515	75	107	31	9
827-02	↓	↓	↓	133	8	[i]6
[c]859-02	↓	↓	↓	3	1	[i]2
A74-022-01	↓	↓	↓	4	2	[i]2
022-02	↓	↓	↓	136	12	[i]8
037-01	↓	↓	↓	126	10	[i]7
[f]037-02	↓	↓	↓	99	5	[i]4
451-01	↓	↓	↓	124	20	11
451-02	↓	↓	↓	141	15	10
234-01	↓	450	65	294	14	[i]5
234-02	↓	450	65	380	13	10
[g]512-01	980	275	40	73	20	--
512-02	980	275	40	83	8	[i]8
198-01	1040	205	30	42	25	11
198-02	↓	205	30	47	24	12
[c, d, j]A73-649-01	↓	150	22	84	22	[i]12
[a, c, h, j]649-02	↓	↓	↓	---	--	--
847-01	↓	↓	↓	170	20	[i]6
847-02	↓	↓	↓	185	20	6
[c]A74-063-01	↓	↓	↓	201	15	12
[c]063-02	↓	↓	↓	240	21	10
[c]069-01	↓	↓	↓	239	15	[i]10
[c]069-02	↓	↓	↓	263	25	17
[f]010-01	↓	↓	↓	184	32	12
010-02	↓	↓	↓	207	21	14
205-01	↓	140	20	322	14	[i]9
205-02	↓	140	20	243	35	14

[a]Short specimen.
[b]Partial head shear.
[c]Tested in helium.
[d]Medium-length specimen.
[e]Failed on loading.
[f]Long specimen, partial head shear.
[g]Lost part of gage, no elongation measurable.
[h]Total head shear, not a valid test.
[i]Failed near end of gage section.
[j]Helium contaminated with oil.

TABLE III. - STRESS RUPTURE AND TENSILE TEST DATA OF $\gamma/\gamma' - \delta$

AFTER BURNER RIG EXPOSURE

Specimen[a]	Batch	Postexposure test conditions			Distance of failure from top of specimen, cm	Rupture life, hr	Ultimate tensile strength		Reduction of area, percent	Elongation, percent
		Temperature, °C	Stress				MN/m^2	ksi		
			MN/m^2	ksi						
A73-865-01	1	760	760	110	4.6	45.9	----	---	3	1
865-02	1	↓	↓	↓	4.3	20.5	----	---	2	1
A74-162-01	2				4.6	69.1	----	---	2	1
162-02	↓				2.3	107.5	----	---	1	2
175-01					4.1	19.6	----	---	9	4
175-02					4.8	111.7	----	---	2	2
597-01	3				2.2	106.4	----	---	1	1
597-02	3				2.5	34.4	----	---	4	2
637-02	3	↓	↓	↓	2.4	32.5	----	---	3	2
A73-858-01	1	1040	150	22	4.6	219.0	----	---	16	13
[b]858-02	1	↓	↓	↓	3.0	215.4	----	---	15	8
A74-171-01	2				2.3	267.4	----	---	15	10
171-02	2				4.8	276.7	----	---	15	8
[b]619-02	3	↓	↓	↓	4.3	310.6	----	---	15	9
A74-169-01	2	760	Tensile		3.8	-----	1015	147	24	16
169-02	2	↓	↓		3.8	-----	945	136	12	6
589-02	3				4.3	-----	960	139	13	9
650-02	3				2.2	-----	995	144	12	7
695-01	3	↓	↓		4.1	-----	950	137	20	10
A73-830-01	1	1040			2.3	-----	640	93	24	12
863-02	1	1040			2.8	-----	620	90	34	13
A74-599-02	3	1040	↓		2.8	-----	670	97	5	4

[a]All long specimens.

[b]Partial head shear.

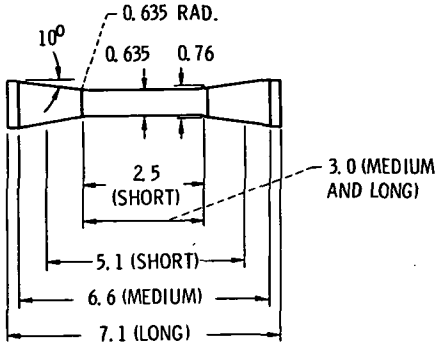

Figure 1. - Taper-headed specimen. (Dimensions are in cm.)

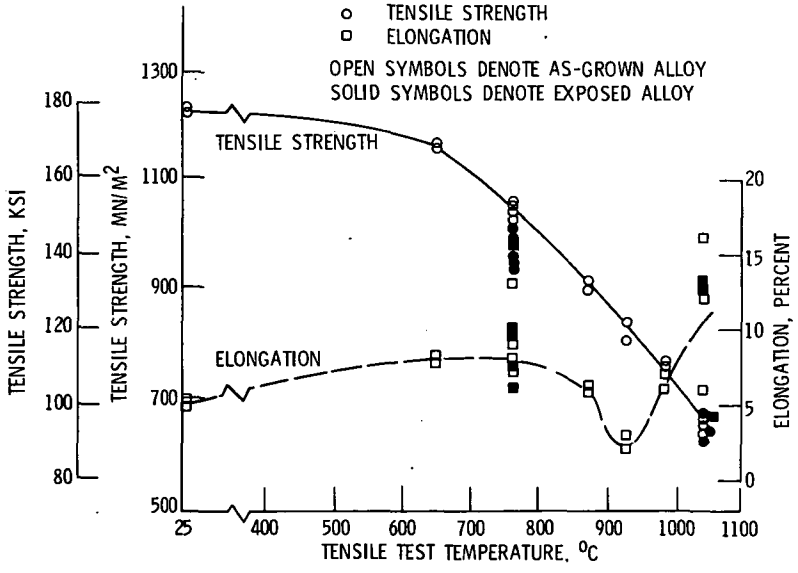

Figure 2. - Effect of cyclic thermal exposure on tensile properties of directionally solidified $\gamma/\gamma' - \delta$ eutectic alloy (Ni-20Cb-6Cr-2.5 Al). Rate of solidification, 3 cm/hr; total cycles from 1100° C to 425° C, 3000; gas velocity, Mach 0.3.

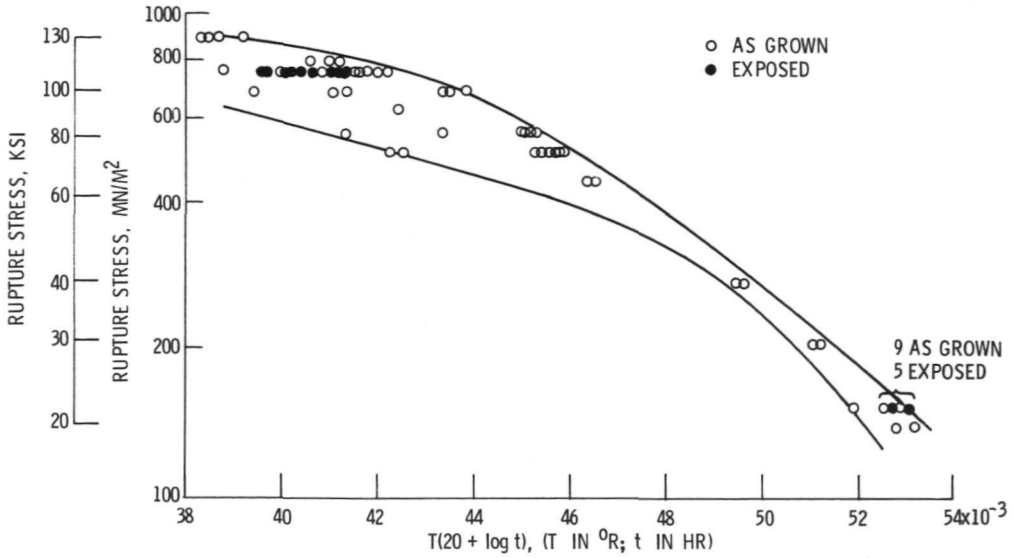

(a) Rupture life.

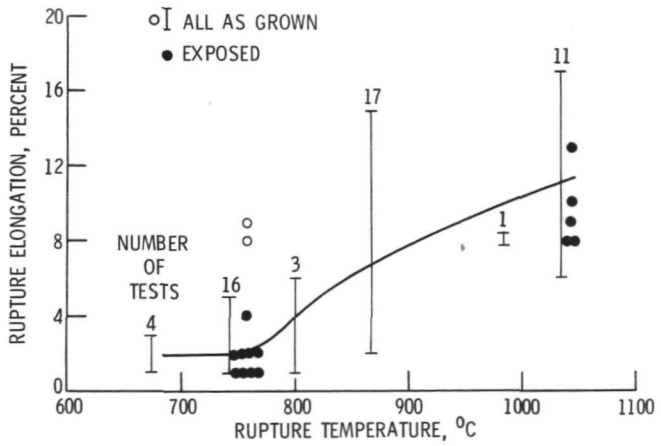

(b) Rupture elongation.

Figure 3. - Effect of cyclic thermal exposure on stress rupture properties of directionally solidified $\gamma/\gamma' - \delta$ eutectic alloy (Ni-20Cb-6Cr-2.5 Al). Rate of solidification, 3 cm/hr; total cycles from 1100^0 C to 425^0 C, 3000; gas velocity, Mach 0.3.

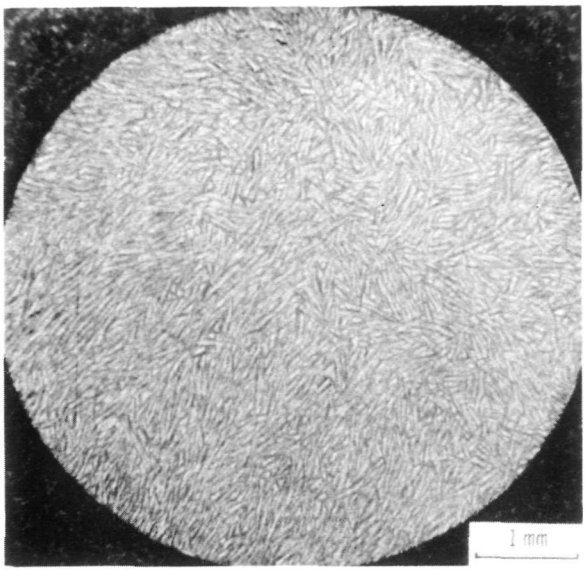

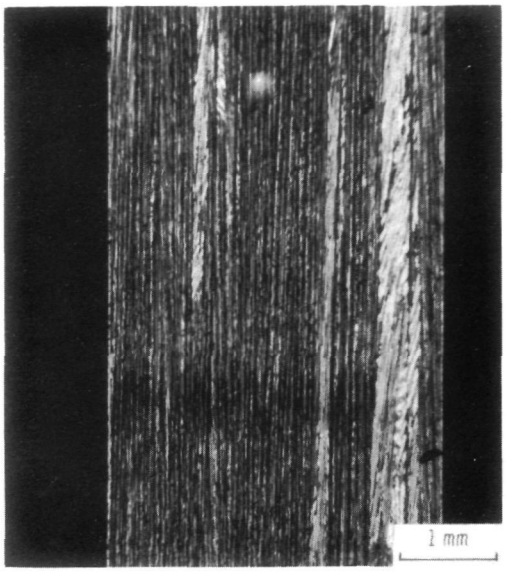

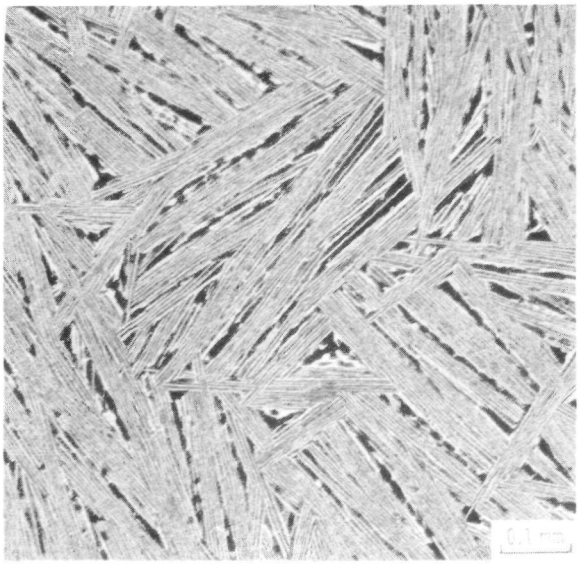

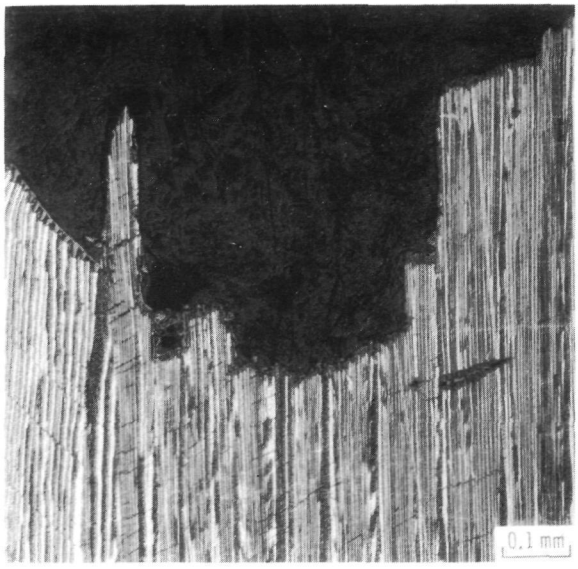

(a) Transverse - near fracture.

(b) Longitudinal.

Figure 4. - Photomicrographs of specimen A73-890-01, as-grown condition. Failure time, 438 hr; stress, 760 MN/m^2 (110 ksi); temperature, 760° C.

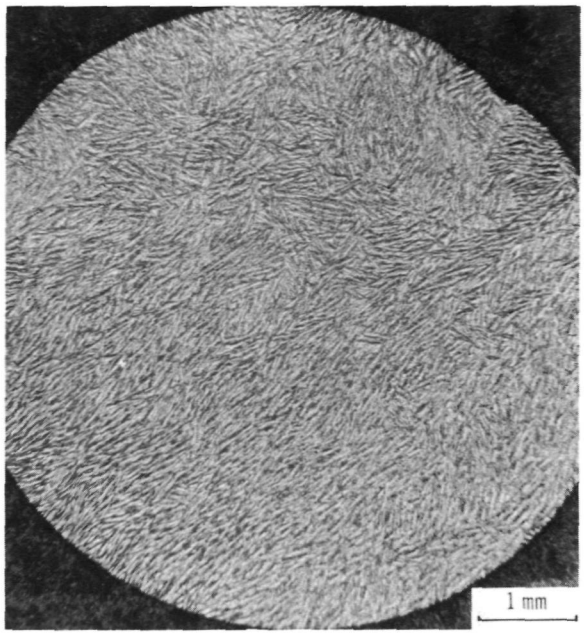

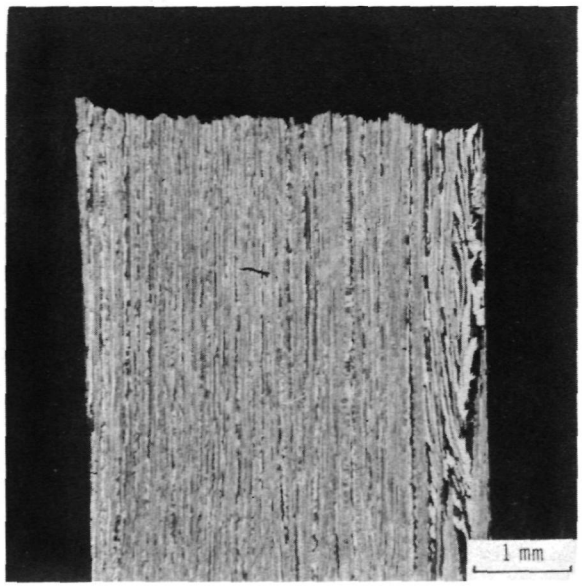

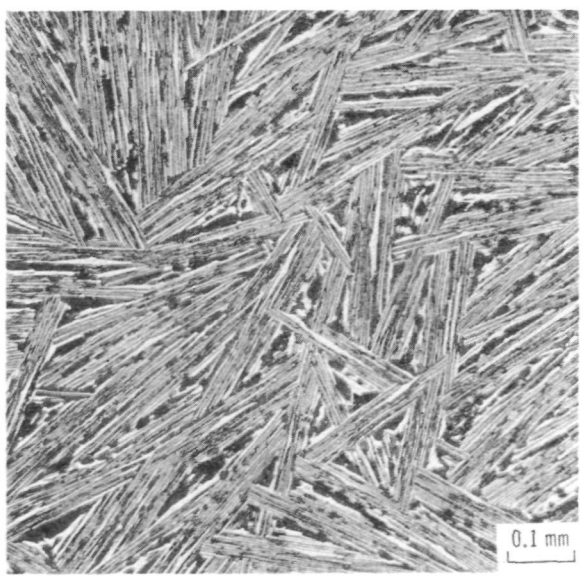

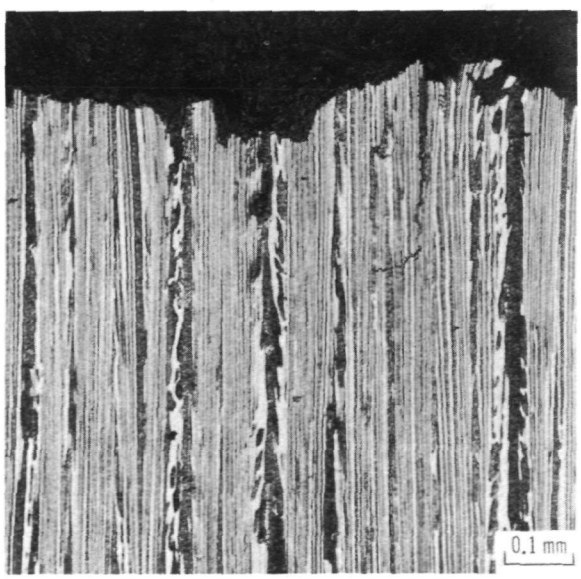

(a) Transverse - near fracture.

(b) Longitudinal.

Figure 5. - Photomicrographs of specimen A73-890-02, as-grown condition. Failure time, 7 hr; stress, 760 MN/m^2 (110 ksi); temperature, 760° C.

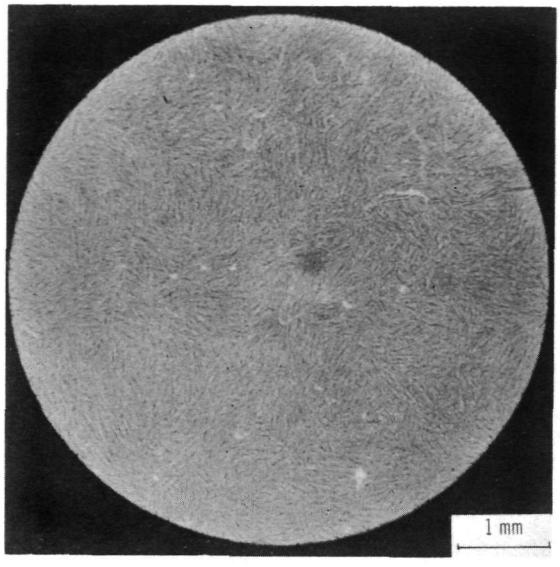

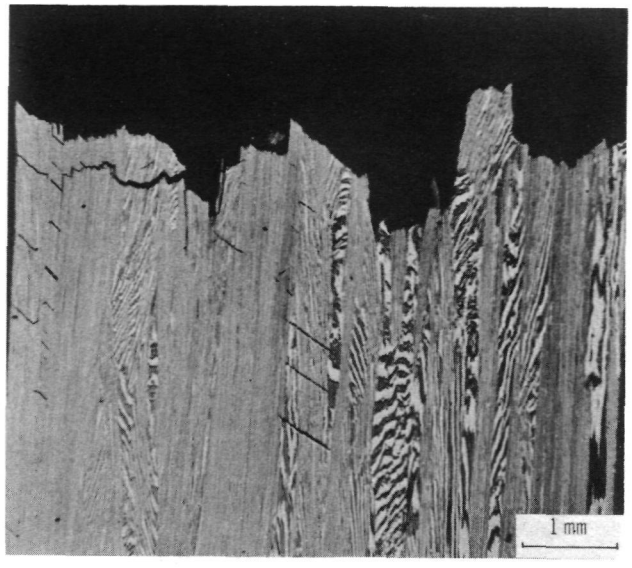

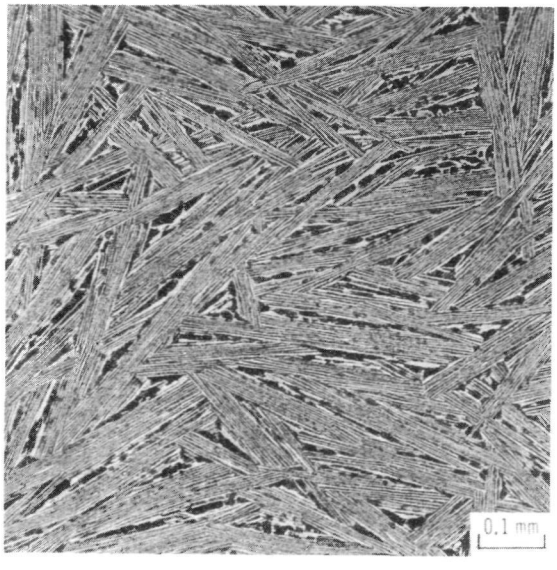

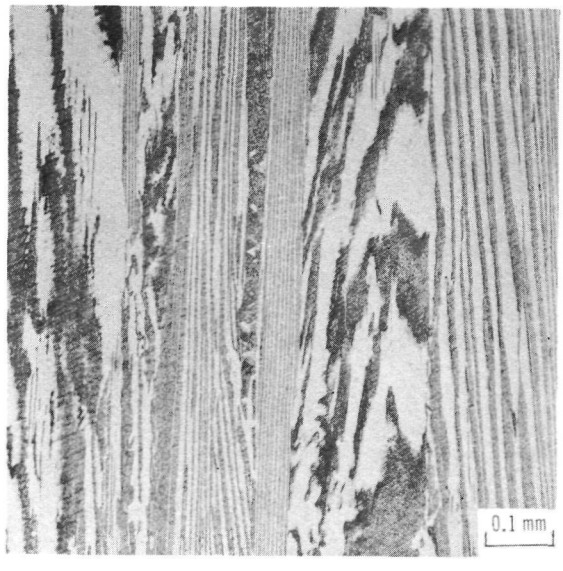

(a) Transverse - near fracture.

(b) Longitudinal.

Figure 6. - Photomicrographs of specimen A74-175-01, after cyclic exposure. Failure time, 19 hr; stress, 760 MN/m^2 (110 ksi); temperature, 760° C.

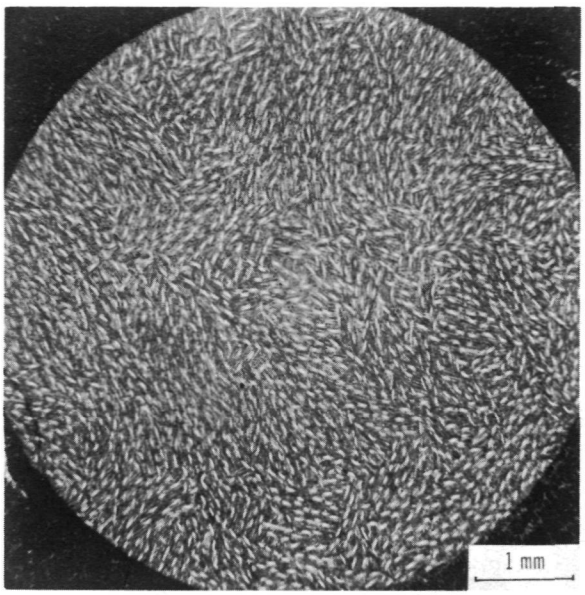

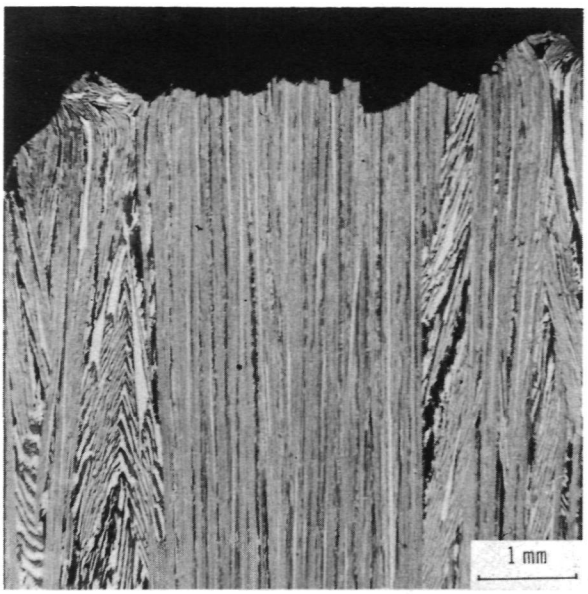

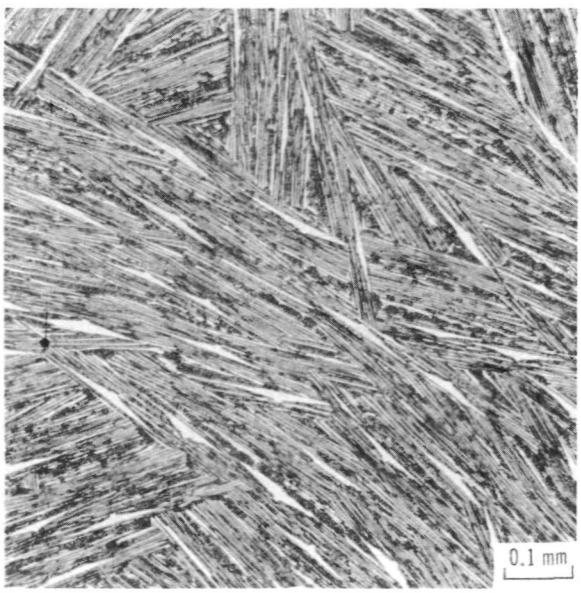

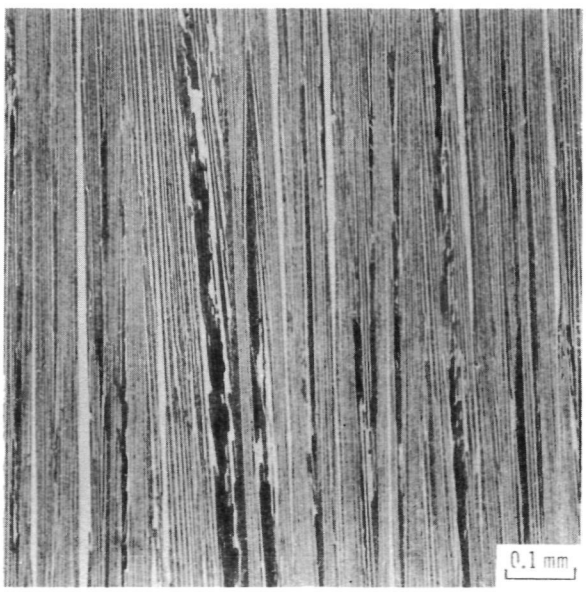

(a) Transverse - near fracture.

(b) Longitudinal.

Figure 7. - Photomicrographs of specimen A74-175-02, after cyclic exposure. Failure time, 111 hr; stress, 760 MN/m^2 (110 ksi); temperature, 760° C.

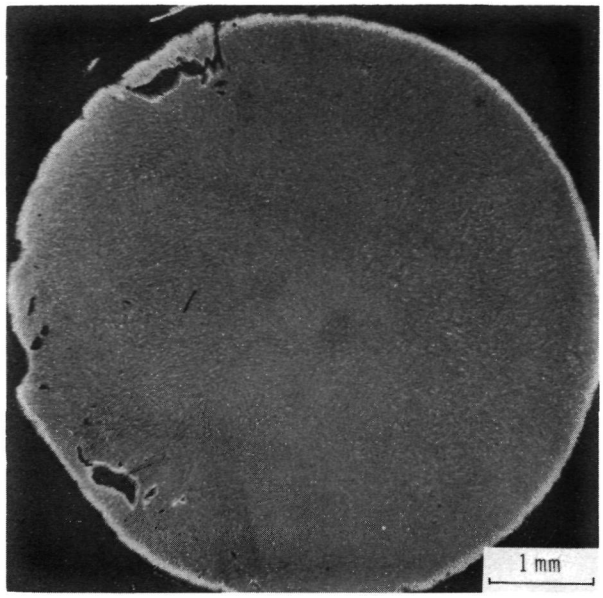

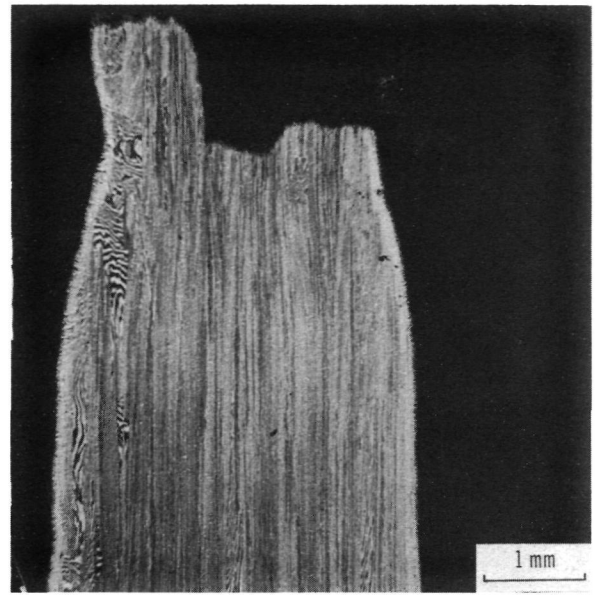

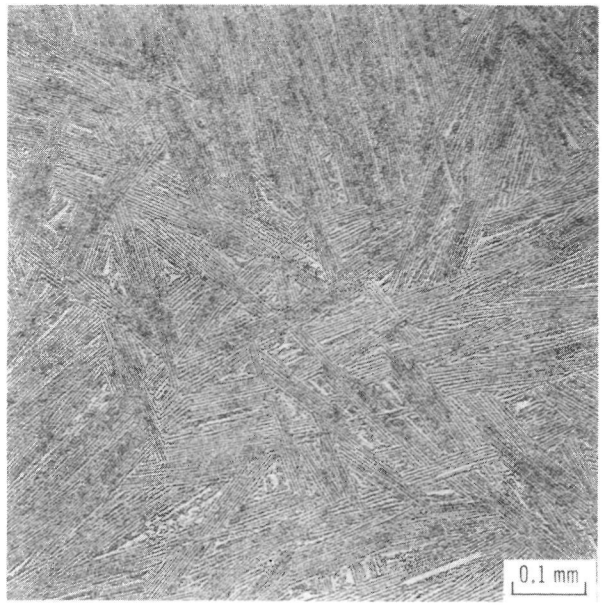

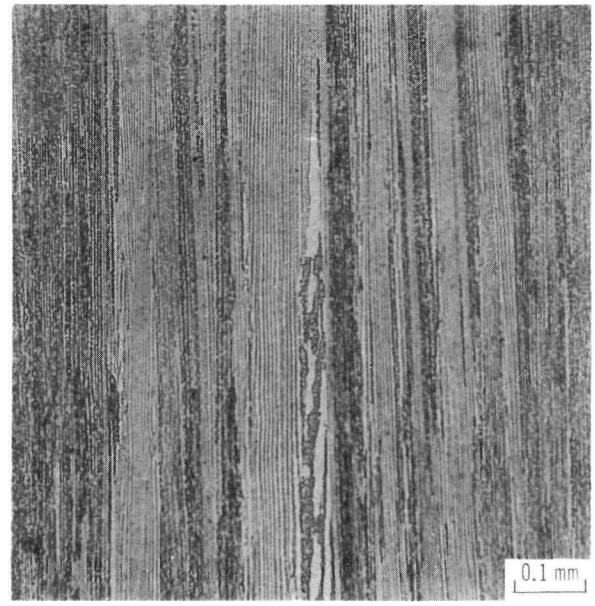

(a) Transverse - near fracture.

(b) Longitudinal.

Figure 8. - Photomicrographs of specimen A74-171-01, after cyclic exposure. Failure time, 267 hr; stress, 150 MN/m^2 (22 ksi); temperature, 1040° C.

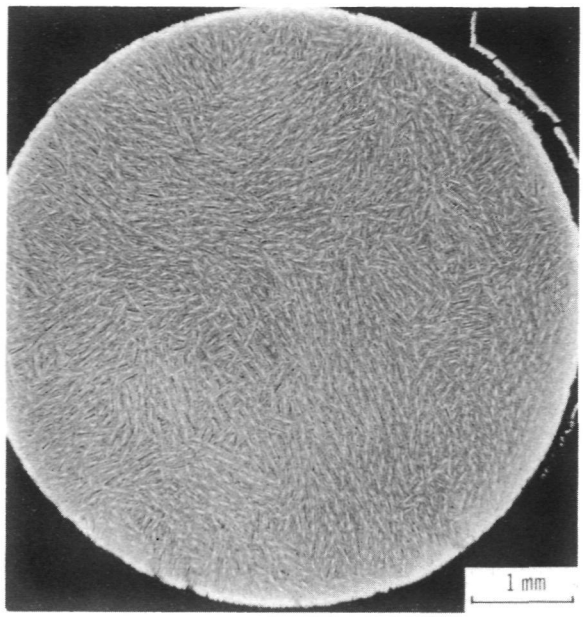

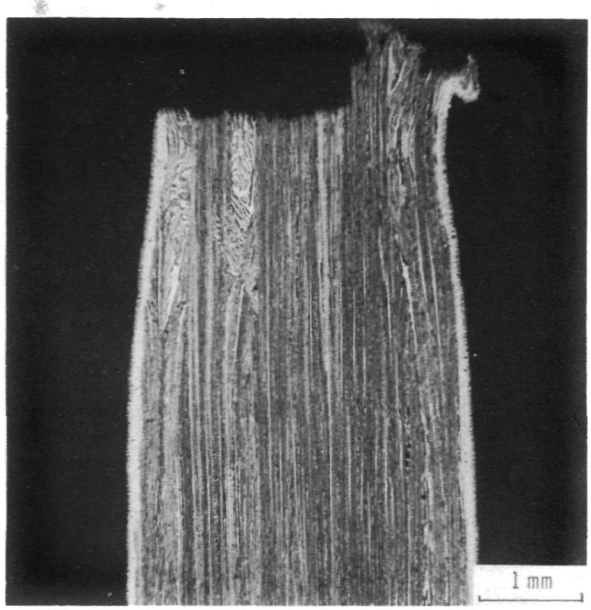

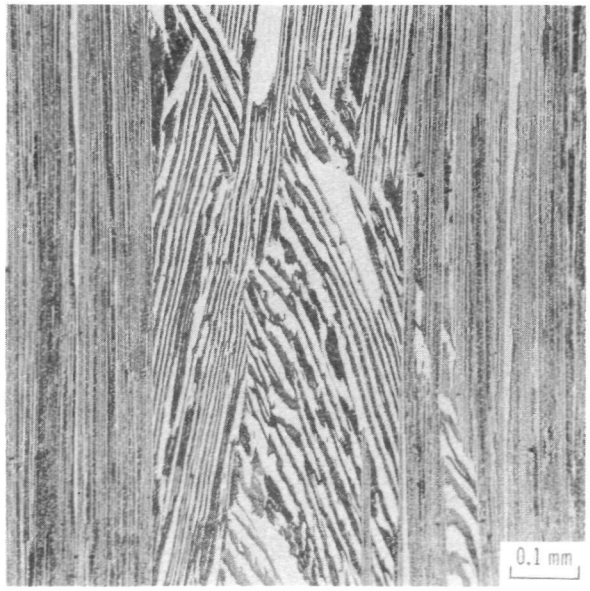

(a) Transverse - near fracture.

(b) Longitudinal.

Figure 9. - Photomicrographs of specimen A74-171-02, after cyclic exposure. Failure time, 276 hr; stress, 150 MN/m^2 (22 ksi); temperature, 1040° C.

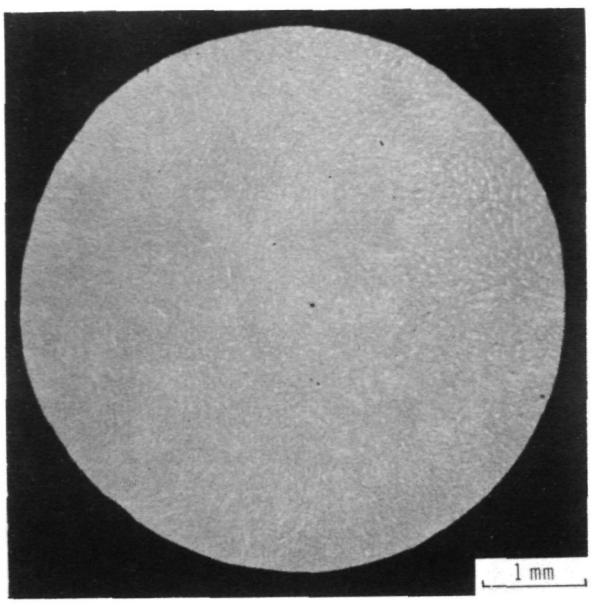

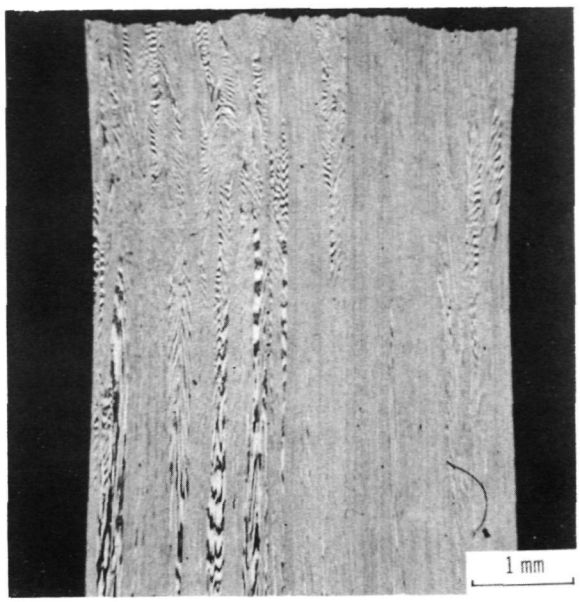

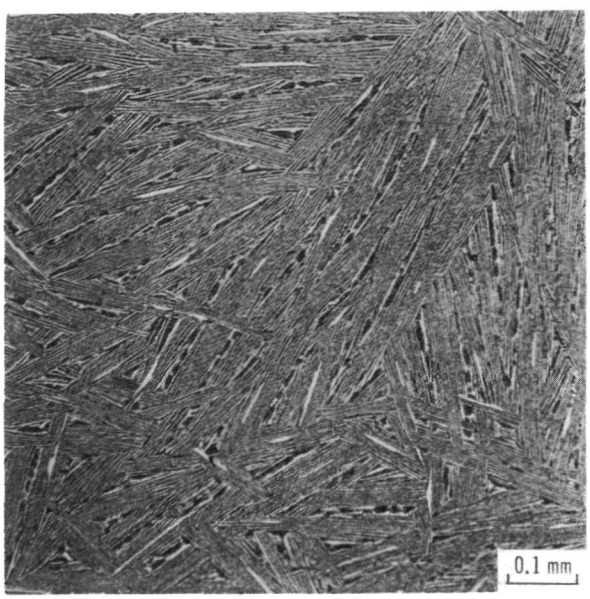

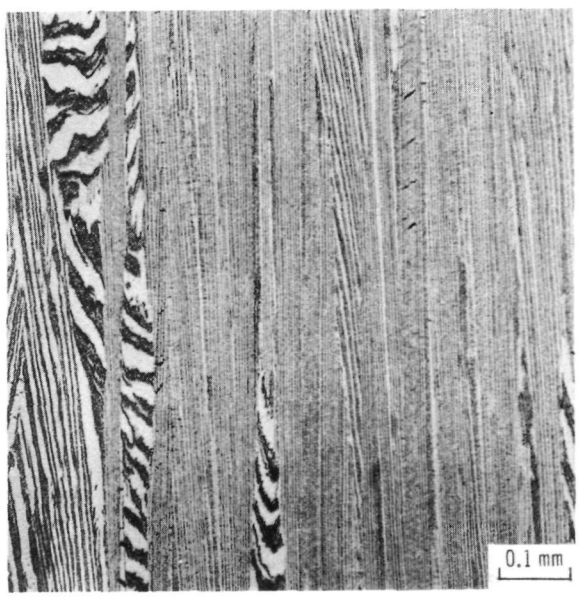

(a) Transverse - near fracture.

(b) Longitudinal.

Figure 10. - Photomicrographs of specimen A74-169-01, after cyclic exposure. Ultimate tensile strength, 1015 MN/m^2 (147 ksi); temperature, 760° C.

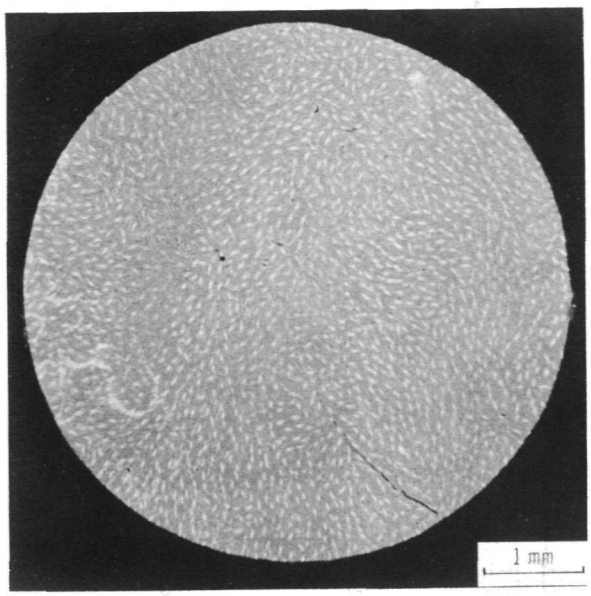

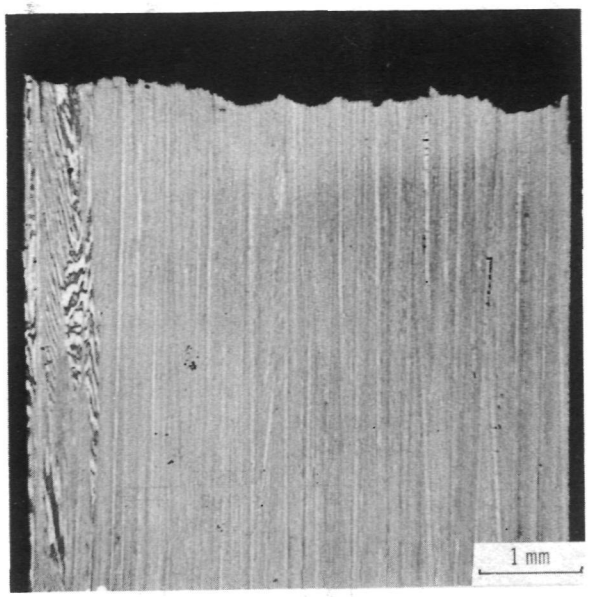

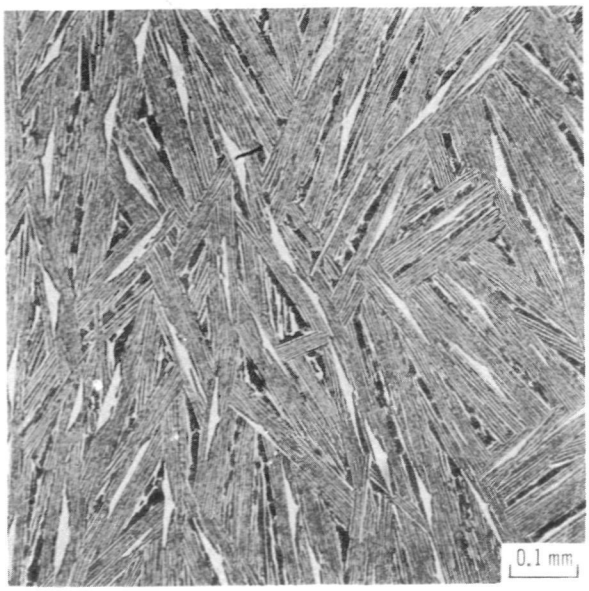

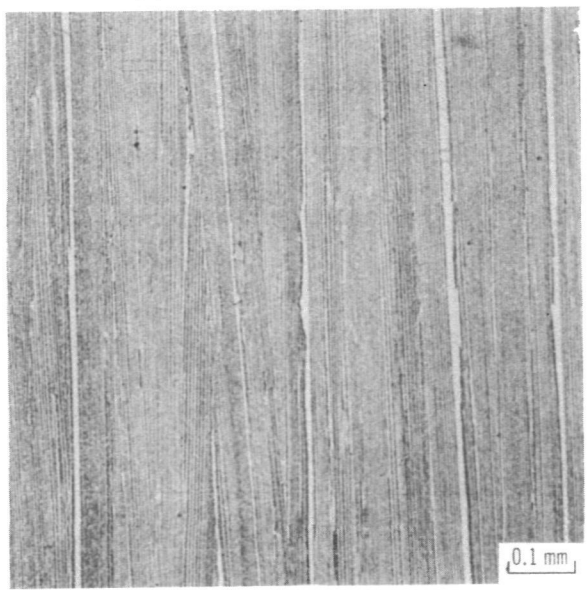

(a) Transverse - near fracture.

(b) Longitudinal.

Figure 11. - Photomicrographs of specimen A74-169-02, after cyclic exposure. Ultimate tensile strength, 945 MN/m^2 (136 ksi); temperature, 760° C.

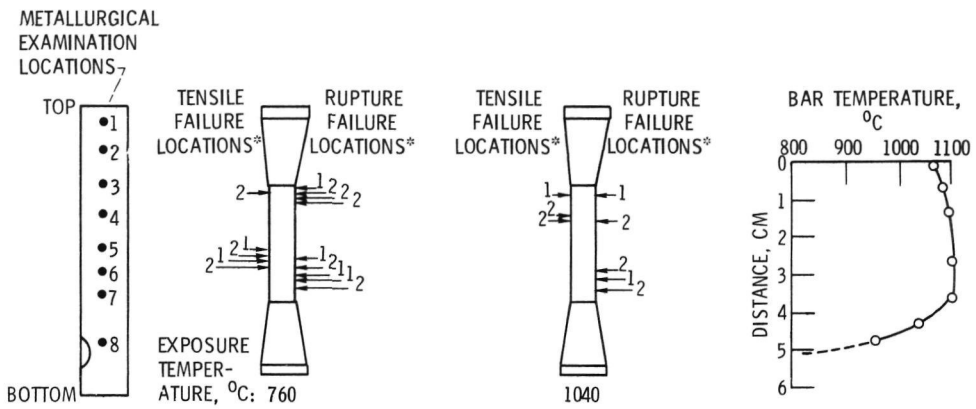

*1 DENOTES BOTTOM BAR OF CASTING; 2 DENOTES TOP BAR OF CASTING.

Figure 12. - Locations of metallurgical examinations, tensile and rupture failures, and thermal profile (ref. 8) of thermally exposed bar.

(a) Transverse - 1; bar temperature, ≈ 1070° C.

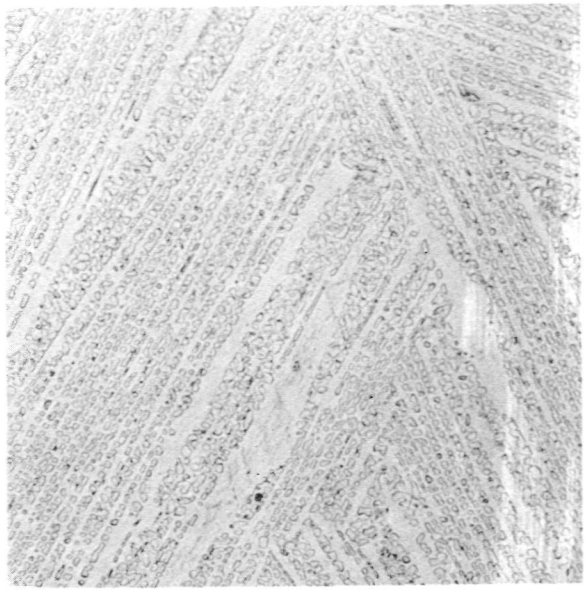

(b) Transverse - 2; bar temperature, 1090° C.

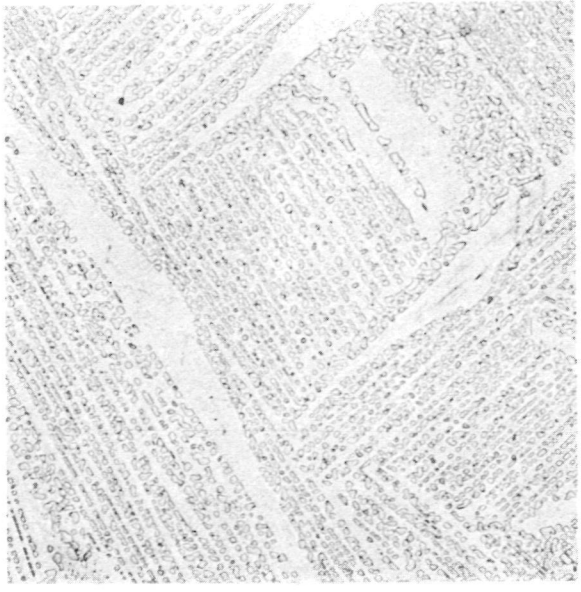

(c) Transverse - 3; bar temperature, 1100° C.

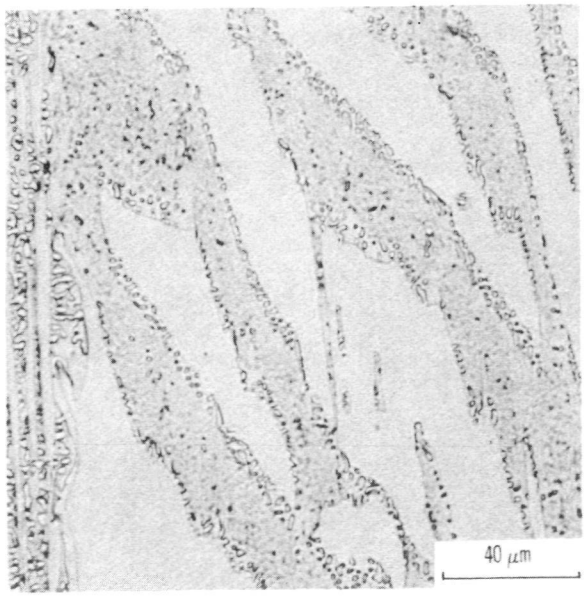

(d) Longitudinal - 2-3; bar temperature, 1090° C.

Figure 13. - Photomicrographs of thermally exposed bar A73-863-01 at positions 1 to 8 (fig. 12).

(e) Transverse - 4; bar temperature, 1100° C.

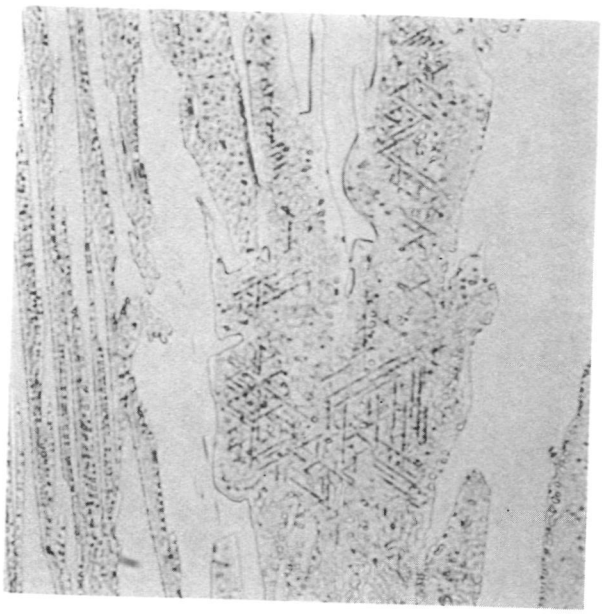

(f) Longitudinal - 3-4; bar temperature, 1100° C.

(g) Transverse - 5; bar temperature, 1080° C.

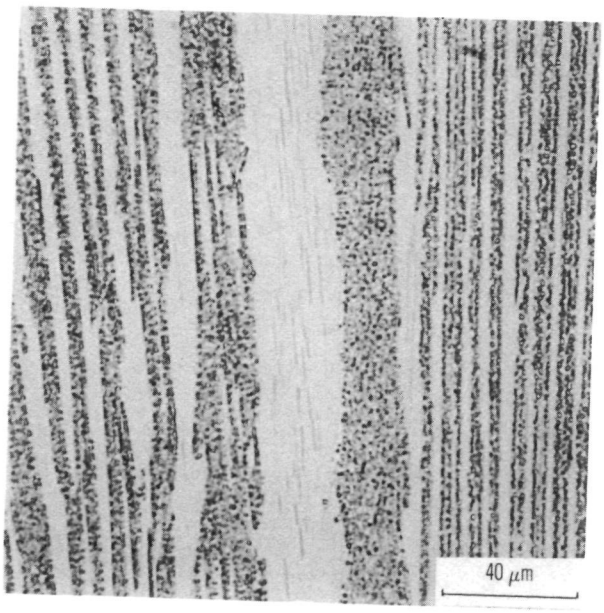

(h) Longitudinal - 4-5; bar temperature, 1080° C.

Figure 13. - Continued.

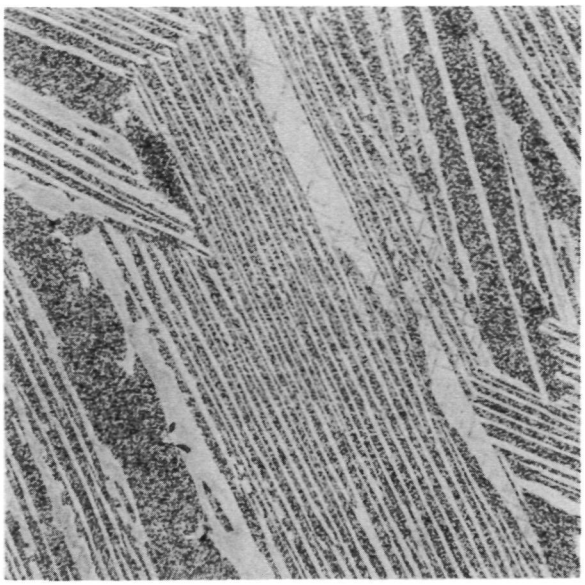

(i) Transverse - 6; bar temperature, 1000° C.

(j) Transverse - 7; bar temperature, 900° C.

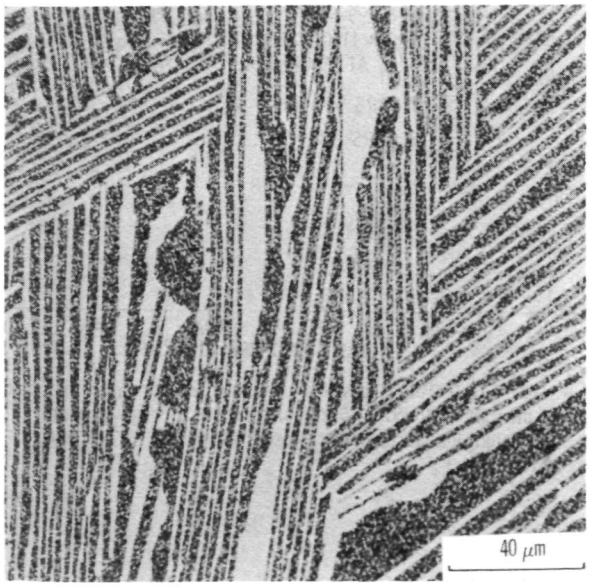

(k) Transverse - 8; bar temperature, 500° C.

Figure 13. - Concluded.

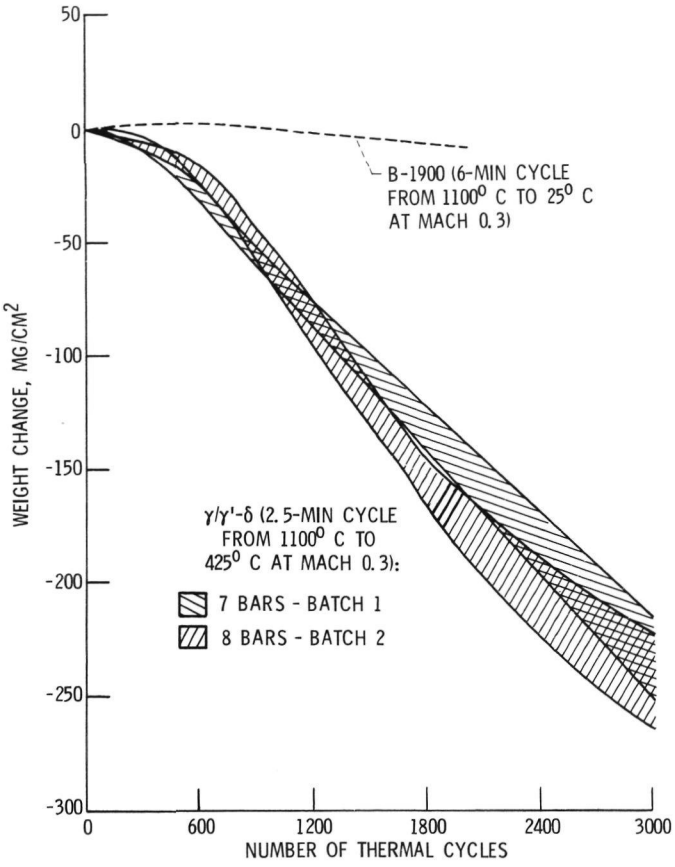

Figure 14. - Weight loss of directionally solidifed γ/γ' - δ eutectic alloy (Ni-20Cb-6Cr-2.5 Al) during cyclic thermal exposure. (Weight loss assumed to be occurring only in top half of bar (15 cm^2).)

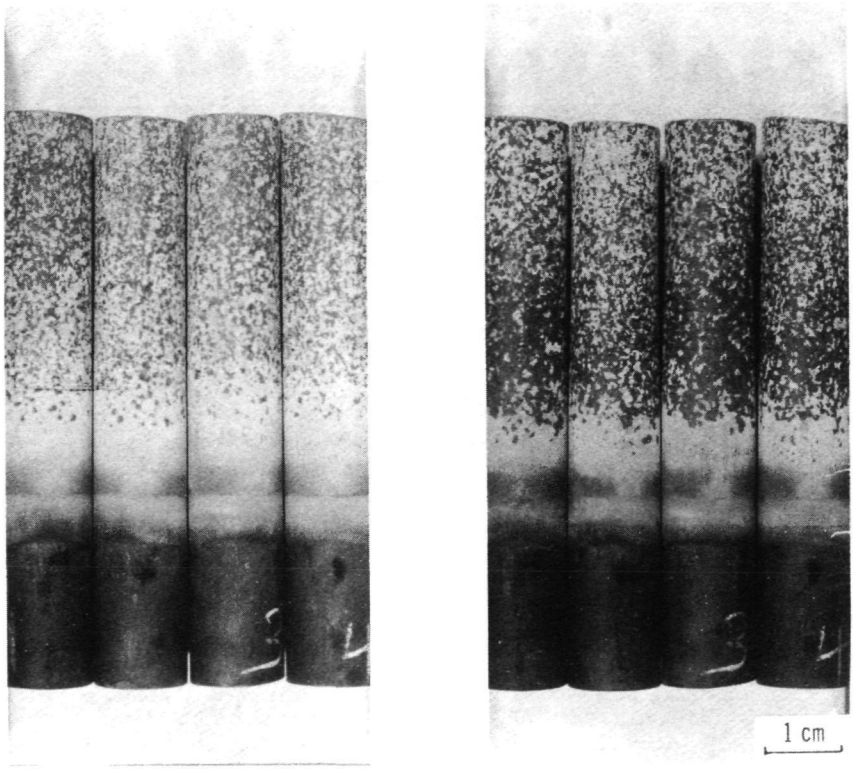

(a) 1500 cycles.

(b) 3000 cycles.

Figure 15. - Test bars after thermal cycling from 1100° C to 425° C at Mach 0.3 gas velocity. (Left to right: A73-830-01, 02; A73-858-01, 02.)

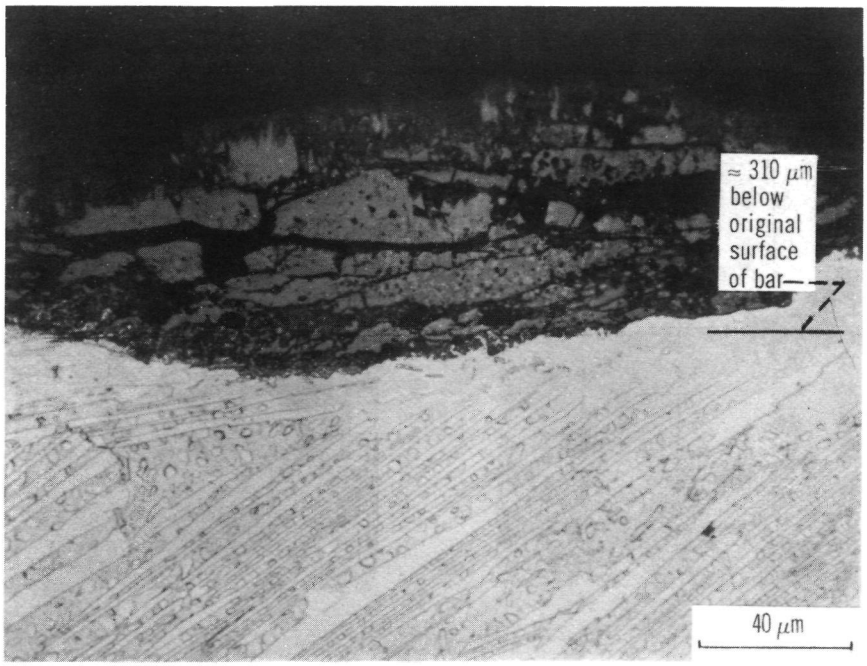

Figure 16. - Transverse section of test bar A73-830-02 after 3000 thermal cycles from 1100° C to 425° C at Mach 0.3 gas velocity.

"The aeronautical and space activities of the United States shall be conducted so as to contribute . . . to the expansion of human knowledge of phenomena in the atmosphere and space. The Administration shall provide for the widest practicable and appropriate dissemination of information concerning its activities and the results thereof."

—NATIONAL AERONAUTICS AND SPACE ACT OF 1958

NASA SCIENTIFIC AND TECHNICAL PUBLICATIONS

TECHNICAL REPORTS: Scientific and technical information considered important, complete, and a lasting contribution to existing knowledge.

TECHNICAL NOTES: Information less broad in scope but nevertheless of importance as a contribution to existing knowledge.

TECHNICAL MEMORANDUMS: Information receiving limited distribution because of preliminary data, security classification, or other reasons. Also includes conference proceedings with either limited or unlimited distribution.

CONTRACTOR REPORTS: Scientific and technical information generated under a NASA contract or grant and considered an important contribution to existing knowledge.

TECHNICAL TRANSLATIONS: Information published in a foreign language considered to merit NASA distribution in English.

SPECIAL PUBLICATIONS: Information derived from or of value to NASA activities. Publications include final reports of major projects, monographs, data compilations, handbooks, sourcebooks, and special bibliographies.

TECHNOLOGY UTILIZATION PUBLICATIONS: Information on technology used by NASA that may be of particular interest in commercial and other non-aerospace applications. Publications include Tech Briefs, Technology Utilization Reports and Technology Surveys.

Details on the availability of these publications may be obtained from:

SCIENTIFIC AND TECHNICAL INFORMATION OFFICE

NATIONAL AERONAUTICS AND SPACE ADMINISTRATION

Washington, D.C. 20546